Non-Linear UWB Receivers With MLSE Post-Detection

Florian Troesch, Thomas Zasowski, and Armin Wittneben
Communication Technology Laboratory, ETH Zurich, 8092 Zurich, Switzerland
Email: {troeschf,zasowski,wittneben}@nari.ee.ethz.ch

***Abstract*— A wireless body area network with an average throughput of 500 kbps is considered based on ultra-wideband (UWB) pulse position modulation. For a long battery autonomy ultra low power consumption is essential. In [1] a FCC compliant ultra low power UWB communication system was presented. By means of a 1% duty cycle at 50 Mbps peak data rate, the power consumption of the system is estimated below $1\,\mathrm{mW}$. To increase inter-symbol interference (ISI) robustness as well as for synchronization, a simple post-detection maximum-likelihood sequence estimator (MLSE) has been presented [2], [3]. In this work, we extend this MLSE approach to over-sampled energy detectors and non-ideal integration windows. Furthermore, we present optimal MLSE metrics based on partial channel state information as a performance benchmark.**

I. Introduction

Recently, ultra-wideband (UWB) wireless body area networks (WBAN) gained much interest due to a multitude of attractive applications, such as wireless health monitoring or ubiquitous computing. In a WBAN, a number of small nodes are placed very close to the human body. Since WBAN nodes get their power from rechargeable batteries, it is inevitable that they are extremely energy efficient. To meet such energy requirements, a low duty cycle operation of the nodes and thus a high peak data rate is essential. An ultra low power UWB communication system has been presented [1] complying with the Federal Communication Commission's (FCC) regulations. With a 1% duty cycle operation realized by a peak data rate of 50 Mbps an average power consumption below $1\,\mathrm{mW}$ can be achieved. Due to low complexity requirements, an orthogonal binary pulse position modulation (BPPM) was considered combined with a simple energy detector (ED).

Due to the high pulse rate of 50 Mbps, even a moderate channel delay spread leads to inter-symbol interference (ISI). This drastically degrades the performance of the ED, which is very sensitive to ISI. For increased ISI robustness and a power efficient symbol synchronization, a simple post-detection maximum likelihood sequence estimator (MLSE) has been presented [2], [3]. The MLSE bases its decision on the output samples of a non-linear frontend which consists of a squaring device and a low pass (LP) filter, which acts as low complexity integration unit. In this work, we extend the system to the case of an over-sampled frontend and estimate the performance increase as a function of over-sampling. Furthermore, a simple but efficient equalization approach is proposed to mitigate ISI effects, introduced by practical low pass filters [1].

In optical communications energy detection based MLSE is well understood [4]. Also publications on MSLE in UWB impulse radio (UWB-IR) can be found [5]. However, linearized system are used and effects of non-linear cross-terms or non-Gaussian distributions are neglected.

The main contribution of this work is the application of the MLSE principle to an over-sampled, non-linear output of an analog UWB BPPM frontend, explicitly taking into account the effect of non-linear cross-correlation terms, data dependent noise variances, non-Gaussian distributions as well as non-ideal integration windows. Different sub-optimal low complexity MLSEs are investigated assuming Gaussian distributed samples at the output of the non-linear frontend. For the cases of instantaneous and average power delay profile (IPDP/APDP) knowledge at the receiver, optimal MLSE metrics are derived. They take into account non-Gaussian distributions and serve as benchmark for the sub-optimal receiver structures. Although the frontend is over-sampled, all MLSEs are implemented as simple Viterbi algorithms which work at symbol rate and with only very few states.

As a next step towards practical receiver realization, the effect of non-ideal LP filters is considered. It is shown that ISI introduced by LP filters of small bandwidth can be removed almost entirely by a simple additional equalizer. As a decreased LP bandwidth reduces synchronization requirements, this equalization is a promising add-on in practical systems. Overall, the presented scheme is a very attractive candidate for ISI mitigation and symbol synchronization in ultra low complexity receivers.

The paper is organized as follows. In Section II, the system model is introduced. The MLSE metrics are evaluated in Sections III and V. The equalizer for non-ideal LP filtering is discussed in Section IV. Performance results are presented in Section VI followed by a short summary in Section VII.

II. Discrete System Model

According to Fig. 1, a real discrete time system model of a UWB-IR with BPPM is considered. It is assumed that only one pulse per bit is transmitted. This is reasonable for short range communication in WBANs due to a moderate path loss [1]. Time-hopping is omitted as a time-division multiple

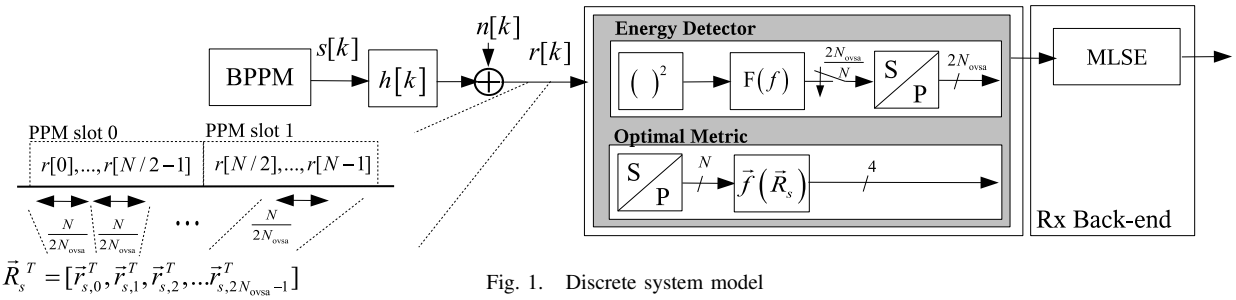

Fig. 1. Discrete system model

access (TDMA) approach is considered. The nominal pulse period N determines a BPPM frame. Each frame contains one transmit pulse. Depending on the BPPM symbol value, the pulse is transmitted either in the first or the second BPPM half-frame of duration $N/2$. The high peak data rate along with a moderate delay spread yields ISI. Mapping the s-th BPPM symbol to a binary vector according to

$$b_s = 0 \rightarrow \vec{x}_s = [\ x_{2s} \quad x_{2s+1}\ ]^T = [\ 1 \quad 0\ ]^T \quad (1)$$
$$b_s = 1 \rightarrow \vec{x}_s = [\ x_{2s} \quad x_{2s+1}\ ]^T = [\ 0 \quad 1\ ]^T, \quad (2)$$

the receive signal becomes

$$r[k] = \sum_s x_{2s} h\left[k - sN\right] + x_{2s+1} h\left[k - sN - \frac{N}{2}\right] + n\left[k\right], \quad (3)$$

with $h[k]$ the discrete channel impulse response (CIR) of the overall system including transmit and receive filter. The channel taps $h[k]$ and the noise samples $n[k]$ are independently Gaussian distributed. The receive signal $r[k]$ is either fed to the sub-optimal energy detector (top) or to the optimal receiver (bottom), whose metric is evaluated directly from the s-th receive vector $\vec{R}_s$ of length N. The output of the ED low pass $F(f)$ is sampled at $2N_{\text{ovsa}}/N$. For notational convenience, the vector $\vec{R}_s$ is divided into $N_{\text{p}} = 2N_{\text{ovsa}}$ parts of $l_{\text{p}} = N/N_{\text{p}}$ samples each, whereby N and N_{ovsa} are chosen such that l_{p} is an integer value:

$$\vec{R}_s = \left[\vec{r}_{s,0}^T, \vec{r}_{s,1}^T, \ldots, \vec{r}_{s,N_{\text{p}}-1}^T\right]^T. \quad (4)$$

This is depicted in Fig. 1, too. The discrete CIR is split accordingly into $N_{\text{p}}L$ parts of l_{p} samples:

$$\vec{h}_s^T = \left[\vec{h}_{s,0}^T, \vec{h}_{s,1}^T, \ldots, \vec{h}_{s,N_{\text{p}}L-1}^T\right]^T, \quad (5)$$

where $L = \lceil N_{\text{h}}/N \rceil$ equals the number of consecutive symbols which are covered by one CIR. Thereby, N_{h} is the maximal number of channel taps. One part of $\vec{R}_s$ is now written as

$$\vec{r}_{s,n} = \sum_{i=0}^{2L-1} \vec{h}_{s-i,n+iN_{\text{ovsa}}} x_{2s+\lfloor \frac{n}{N_{\text{ovsa}}} \rfloor - i} + \vec{n}_{s,n}, \quad (6)$$

where $\vec{n}_{s,n}$ is jointly Gaussian with $\mathcal{E}\left\{\vec{n}_{s,n}\vec{n}_{s,n}^T\right\} = \sigma^2\mathbf{I}$.

III. MLSE for Over-sampled Energy Detectors

In an ideal ED frontend, the impulse response of the filter $f[k]$ is realized as rectangular window of length l_{p}. Hence, the frontend splits each BPPM symbol into N_{p} parts and generates the observation vector

$$\vec{L}_s = \left[L_{s,0}, \ldots, L_{s,N_{\text{p}}-1}\right]. \quad (7)$$

The n-th sample of the s-th symbol at the ED output equals:

$$L_{s,n} = \sum_{i=0}^{2L-1} \sum_{j=0}^{2L-1} \hat{C}_{s,n,i,j} \hat{X}_{s,n,i,j} + z_{s,n} + q_{s,n}, \quad (8)$$

with

$$\hat{C}_{s,n,i,j} = \vec{h}_{s-i,n+iN_{\text{ovsa}}}^T \vec{h}_{s-j,n+jN_{\text{ovsa}}} \quad (9)$$
$$\hat{X}_{s,n,i,j} = x_{2s+\lfloor \frac{n}{N_{\text{ovsa}}} \rfloor - i} x_{2s+\lfloor \frac{n}{N_{\text{ovsa}}} \rfloor - j}, \quad (10)$$

and

$$z_{s,n} \sim \mathcal{N}\left(0, 4\sigma^2 \sum_{i=0}^{2L-1} \sum_{j=0}^{2L-1} \hat{C}_{s,n,i,j} \hat{X}_{s,n,i,j}\right) \quad (11)$$
$$q_{s,n} \sim \chi^2\left(\frac{N}{2N_{\text{ovsa}}}\sigma^2, \frac{N}{N_{\text{ovsa}}}\sigma^4\right), \quad (12)$$

where χ^2 has $\frac{N}{2N_{\text{ovsa}}}$ degrees of freedom. The presented MLSE post-detectors have only limited CSI. In detail, three different MLSEs are considered. MLSE-C1 and MLSE-C2 are based on instantaneous channel knowledge. MLSE-C1 knows the instantaneous correlation matrix $\mathbf{C}_1 = \hat{\mathbf{C}}_s$ with $\hat{\mathbf{C}}_{s,\alpha,\beta} = \vec{h}_{s,\alpha}^T \vec{h}_{s,\beta}$. MLSE-C2 knows only the diagonal values of $\mathbf{C}_1$ and assumes that the cross-correlations are zero, i.e., $\mathbf{C}_2 = \mathbf{I}[\vec{h}_{s,0}^T \vec{h}_{s,0}, \vec{h}_{s,1}^T \vec{h}_{s,1}, \ldots, \vec{h}_{s,N_{\text{p}}L-1}^T \vec{h}_{s,N_{\text{p}}L-1}]$. MLSE-C3 is based on average power knowledge. As we assume independently distributed channel taps $\mathbf{C}_3 = \mathcal{E}\{\mathbf{C_1}\} = \mathcal{E}\{\mathbf{C_2}\}$ is diagonal.

Conditioned on their CSI, the MLSEs assume Gaussian distributed samples at the output of the integrator $F(f)$. This approximation is justified by the Central Limit theorem due to the large number of samples in the summation. Furthermore, they assume no correlation between the samples $L_{s,n}$, conditioned on the CSI. This is correct for MLSE-C1 and MLSE-C2 as they have instantaneous CSI but not for MLSE-C3. All the same MLSE-C3 performs well. All considered MLSEs are realized by Viterbi algorithms maximizing:

$$\underset{\vec{b}}{\text{argmax}} \sum_s \log\left(p\left(\vec{L}_s | b_s, b_{s-1}, \ldots, b_{s-L+1}, \mathbf{C}\right)\right), \quad (13)$$

with

$$\log\left(p\left(\vec{L}_s|b_s,b_{s-1},\ldots,b_{s-L+1},\mathbf{C}\right)\right) = \sum_{n=0}^{N_\mathrm{p}-1} -0.5\log\left(2\sigma_{s,n}^2\pi\right) - \frac{|L_{s,n}-m_{s,n}|^2}{2\sigma_{s,n}^2}, \quad (14)$$

and

$$m_{s,n} = \sum_{i=0}^{2L-1}\sum_{j=0}^{2L-1}\hat{C}_{s,n,i,j}\hat{X}_{s,n,i,j} + \frac{N}{2N_\mathrm{ovsa}}\sigma^2 \quad (15)$$

$$\sigma_{s,n}^2 = \sigma^2\sum_{i=0}^{2L-1}\sum_{j=0}^{2L-1}\hat{C}_{s,n,i,j}x_{s,n,i,j} + \frac{N}{N_\mathrm{ovsa}}\sigma^4. \quad (16)$$

Increasing the over-sampling rate N_ovsa inherently increase the channel estimation effort.

IV. Equalizing Practical Low Pass Filters

By now the integration was done by an ideal rectangular window of $l_\mathrm{p} = N/N_\mathrm{p}$ samples, i.e., no additional ISI was introduced by the LP. If the integration is realized by a realistic LP filter, e.g., a first order LP filter, significant ISI can occur. Fortunately, the LP introduces correlation to signal and noise component exactly the same way as it is located after the amplifiers and the additive noise. For certain types of LP filters, we show that a simple zero-forcing (ZF) equalization is optimal in the sense that it entirely removes ISI without any performance loss and demonstrate its effectiveness in practice. In detail, we consider low pass filters of the form

$$f[k] = \sum_d f_d w_{\frac{N}{N_\mathrm{p}}}\left(k - d\frac{N}{N_\mathrm{p}}\right), \quad (17)$$

with

$$w_M[n] = \begin{cases} 1 & 0\le n\le M \\ 0 & \text{else}\end{cases}, \quad (18)$$

and the filter coefficients f_d. The correlated output of the ED can therefore be described by:

$$\tilde{L}_n = \sum_d f_d L_{n-d}. \quad (19)$$

This correlation can be entirely removed using a simple ZF equalizer in the digital domain without any performance. Although analog filters described by (17) are hardly realizable in practice, a realistic LP filter of small bandwidth can be approximated pretty well by such a filter characteristic and can be equalized efficiently in the digital domain. Hence, a first order LP and a simple equalizer lead to an ultra low power implementation of an almost perfectly rectangular integration window. The equalization can also be integrated directly into the MLSE metric. However, this is omitted due to notational clarity.

V. Optimal MLSE Receivers In Fast Fading

In this section, we present two Viterbi algorithms for the cases, where the receiver has access to the linear vector $\vec{R}_s$ and knows the overall IPDP or APDP, respectively. They are considered as benchmark for the sub-optimal but much simpler over-sampled energy detection MLSE. The metrics have been evaluated by splitting up the symbolwise ML metrics presented in [3]. For clarity, we restrict our attention to one slot interference, where the discrete channel can be split into a signal component $\vec{v}_s$ and an interfering component $\vec{g}_s$ of length $N/2$ each:

$$\vec{h}_s^T = \left[\vec{v}_s^T, \vec{g}_s^T\right]. \quad (20)$$

As shown in Fig.1, the Viterbi uses the metric $\vec{f}(\vec{R}_s)$, which is based on $\vec{R}_s$ from (4), the partial CSI $\mathcal{C}$ and the previous bit. This leads to:

$$\underset{\vec{b}}{\operatorname{argmax}}\sum_s \log\left(p\left(\vec{R}_s|b_s,b_{s-1},\mathcal{C}\right)\right). \quad (21)$$

In fast fading, the observation vector $\vec{R}_s$ is independent of the past if b_{s-1} and $\mathcal{C}$ are known. Therefore, the presented Viterbi algorithms are optimal MLSEs.

A. Optimal Metric Based on APDP

We split the APDP $\vec{\lambda}_h$ into two parts $\vec{\lambda}_h = \left[\vec{\lambda}_v^T, \vec{\lambda}_g^T\right]^T$ with:

$$\vec{\lambda}_v^T = \mathcal{E}\left\{\left[v_{s,0}^2,,\ldots,v_{s,N/2-1}^2\right]\right\} \quad (22)$$

$$\vec{\lambda}_g^T = \mathcal{E}\left\{\left[g_{s,0}^2,,\ldots,g_{s,N/2-1}^2\right]\right\}, \quad (23)$$

and reorder the observation vector $\vec{R}_s$ according to

$$\vec{d}_s = \left[r_{s,0}, r_{s,N/2}, r_{s,1}, r_{s,N/2+1},\ldots,r_{s,N/2-1}, r_{s,N-1}\right]. \quad (24)$$

With this, the a-posteriori probability of the observation $\vec{d}_s$ or equivalently $\vec{R}_s$ can be described by:

$$p\left(\vec{d}_s|b_s,b_{s-1},\vec{\lambda}_v,\vec{\lambda}_g\right) = \left(\frac{1}{\sqrt{2\pi}}\right)^N\frac{1}{\sqrt{\Delta_d}}\exp\{G\}, \quad (25)$$

with

$$G = -\frac{1}{2}\sum_{k=0}^{N/2-1} r_k^2\lambda_{d,2k,2k}^{-1} + r_{k+N/2}^2\lambda_{d,2k+1,2k+1}^{-1} + 2r_k r_{k+N/2}\lambda_{d,2k,2k+1}^{-1}. \quad (26)$$

The determinant is:

$$\Delta_d = \left(\frac{1}{16}\right)^{\frac{N}{2}}\prod_{j=0}^{N/2-1}\Psi_j, \quad (27)$$

with

$$\Psi_j = 16\sigma^4 + 16\lambda_{v,j}\lambda_{g,j}\left(b_{s-1}b_s + (1-b_s)\right) + 16\lambda_{g,j}\sigma^2\left(b_{s-1} + (1-b_s)\right) + 16\lambda_{v,j}\sigma^2\left(b_s + (1-b_s)\right). \quad (28)$$

The diagonal elements of the inverse equal:

$$\lambda_{d,k,k}^{-1} = \frac{16\left(\lambda_{g,\lceil k/2\rceil}\left(1-b_s\right)+\lambda_{v,\lceil k/2\rceil}b_s+\sigma^2\right)}{\Psi_{\lceil k/2\rceil}}, \quad (29)$$

for k even and

$$\lambda_{d,k,k}^{-1} = \frac{16\left(\lambda_{g,\lceil k/2\rceil}b_{s-1}+\lambda_{v,\lceil k/2\rceil}\left(1-b_s\right)+\sigma^2\right)}{\Psi_{\lceil k/2\rceil}}, \quad (30)$$

for k odd. The non-zero off-diagonal elements are:

$$\lambda_{d,k,k+1}^{-1} = \lambda_{d,k+1,k}^{-1} = -\frac{16\lambda_{g,\lceil k/2\rceil}b_{s-1}\left(1-b_s\right)}{\Psi_{\lceil k/2\rceil}}, \quad (31)$$

whereby k is even. In case of fast fading, the cross-correlation terms vanish and the metric simplifies to:

$$\Delta_d = \prod_{k=0}^{N-1}\lambda_{h,k} \quad (32)$$

$$\lambda_{d,k,k}^{-1} = 1/\lambda_{h,k} \quad (33)$$

$$G = -\frac{1}{2}\sum_{k=0}^{N-1}\frac{r_k^2}{\lambda_{h,k}}. \quad (34)$$

Under the assumption of fast fading and independently distributed Gaussian channel taps, this metric equals the optimal sequence detector and is nearly bit error rate (BER) optimal.

B. Optimal Metric Based on IPDP

For evaluation of the IPDP metric, we split the probability

$$p\left(\vec{R}_s|b_s,b_{s-1},\mathcal{C}_{\text{IPDP}}\right) = \prod_{k=0}^{N/2-1} p\left(r_{s,k},r_{s,k+N/2}|b_s,b_{s-1},x_k,u_k\right), \quad (35)$$

with $\vec{x}$ and $\vec{u}$ the amplitudes of $\vec{v}$ and $\vec{g}$, respectively. If the IPDP is known to the receiver and the phase, i.e., the polarity of the multi-paths changes from symbol to symbol, presented Viterbi algorithm is optimal. For the sake of clarity, it is assumed that the IPDP stays constant over one burst, leading to following metric:

$$\begin{aligned} p\left(r_{s,k},r_{s,k+N/2}|b_s,b_{s-1},x_k,u_k\right) = \\ \frac{1}{4\pi\sigma^2}\exp\left\{-\frac{1}{2\sigma^2}\left[r_{s,k}^2+r_{s,k+N/2}^2+x_k^2\right.\right. \\ \left.\left.+u_k^2\left[b_{s-1}+\left(1-b_s\right)\right]\right]\right\} \\ \left[\cosh\left(\frac{1}{\sigma^2}\left[\left(1-b_{s-1}\right)r_{s,k}u_k+b_sr_{s,k+N/2}u_k\right.\right.\right. \\ \left.\left.\left.+b_sr_{s,k}x_k+\left(1-b_s\right)r_{s,k+N/2}x_k\right]\right)\right. \\ \left.\exp\left\{-\frac{1}{\sigma^2}\left[b_s\left(1-b_{s-1}\right)x_ku_k\right]\right\}+\right. \\ \cosh\left(\frac{1}{\sigma^2}\left[\left(1-b_{s-1}\right)r_{s,k}u_k+b_sr_{s,k+N/2}u_k\right.\right. \\ \left.\left.-b_sr_{s,k}x_k-\left(1-b_s\right)r_{s,k+N/2}x_k\right]\right) \\ \left.\exp\left\{\frac{1}{\sigma^2}\left[b_s\left(1-b_{s-1}\right)x_ku_k\right]\right\}\right]. \end{aligned} \quad (36)$$

VI. Performance

To see the impact of over-sampling and LP filtering, we compare the performance of different MLSEs by means of BER simulations. The BER is plotted over the signal-to-noise ratio E_b/N_0, where E_b denotes the energy per bit and $N_0/2$ is the noise power spectral density. We assume uniformly distributed channel taps, which is a kind of worst case scenario for a given delay spread. To achieve a data rate of 50 Mbps with BPPM, one bit has to be transmitted every 20 ns. A BPPM frame has a duration of $T = 20$ ns and a half-frame a duration of 10 ns. Hence, ISI occurs for CIRs with a duration of more than $\tau = 10$ ns. To investigate the performance gains achievable by over-sampling, moderate and strong ISI are considered assuming an ideal integration window. In case of moderate ISI the CIR has a duration of $\tau = 14$ ns and in case of strong ISI $\tau = 19$ ns.

a) Moderate ISI: In Fig. 2, the performance of the MLSE-C2 (instantaneous without cross-terms) and MLSE-C3 (average) is shown for different over-sampling factors N_ovsa. As benchmark, the performance curves of the significantly more complex but optimal MLSE-APDP and MLSE-IPDP are given. The performance of the symbolwise ED is indicated as well and demonstrates its high sensitivity even to moderate ISI. Already the very limited CSIs $\mathbf{C}_2$ or $\mathbf{C}_3$ without over-sampling lead to significant performance improvement. But both MLSE-APDP and MLSE-IPDP show still significantly better performance highlighting that there is still space for improvement. A small over-sampling factor $N_\text{ovsa} = 2$ brings again a large performance gain for both MLSE-C2 and MLSE-C3. The performance of the MLSE-C3 does not improve further by increasing the over-sampling factor to $N_\text{ovsa} > 2$. This is due to the fact that the uniform APDP with $\tau = 14$ ns can be described almost perfectly by 3 integration parts of $T_\text{int}/N_\text{ovsa} = 5$ns duration. Depending on the APDP at hand, higher over-sampling can still bring improvements in other scenarios. The performance gap between the MLSE-C3 and the MLSE-APDP is due to the non-Gaussian distribution and the correlation between first and second half-frame considered in the MLSE-APDP metric. The MLSE-C2 further improves with higher over-sampling and for $N_\text{ovsa} = 12$ achieves almost the same performance as the much more complex MLSE-APDP.

b) Strong ISI: For a uniform APDP with $\tau = 19$ ns, the MLSE-C3 performance does not improve significantly with over-sampling, as the APDP over two PPM slots is almost flat. This is shown in Fig. 3. The MLSE-C3 does hardly improve even for an over-sampling of $N_\text{ovsa} = 60$. MSLE-C1 and MLSE-C2 improve steadily with increasing sampling rate. Although the over-sampling gains do not seem very large on first glance, there is still a SNR difference of about 4 dB between $N_\text{ovsa} = 1$ and $N_\text{ova} = 120$ at a BER $= 10^{-3}$ and much larger gains can be expected for non-uniform APDPs. The performance gap of 3 dB between MLSE-C2 with $N_\text{ovsa} = 120$ and the MLSE-IPDP arises

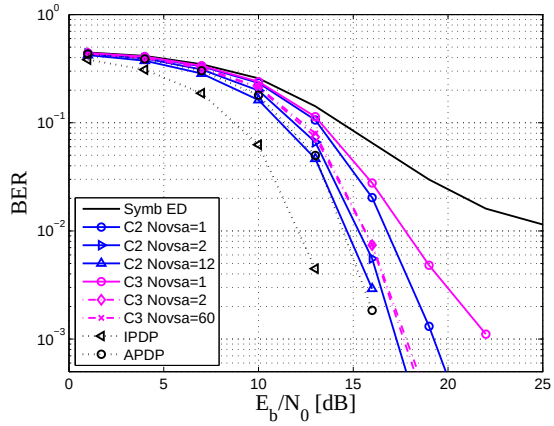

Fig. 2. BER performance in case of moderate ISI ($\tau = 14$ ns)

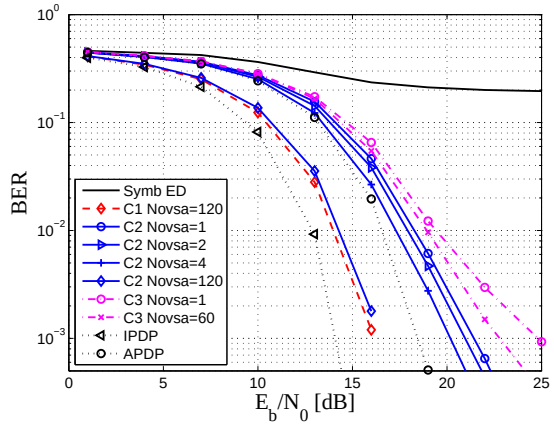

Fig. 3. BER performance in case of strong ISI ($\tau = 19$ ns)

due to the Gaussian assumption made for the metric of the MLSE-C2, which looses its appropriateness with increasing over-sampling. The consideration of the cross-terms in the metric of C1 does not improve the performance significantly compared to MLSE-C2. This agrees with earlier findings for $N_{\text{ovsa}} = 1$. It was found that the cross-terms bring only small improvement for ISI below 20 ns [2].

The performance of the MLSE-APDP depends much on the amount of information contained in the APDP. If the APDP is the result of averaging over very different channels, the APDP is very different from the IPDP and contains hardly useful information. In this case, the MLSE-APDP approaches the MLSE-ED. However, if the APDP results from averaging over rather similar channels, such as in a slow fading scenario, the APDP resembles pretty much the IPDP and contains a lot of useful information. In this case, the MLSE-APDP approaches the MLSE-IPDP. UWB is basically an indoor technology, where slow fading scenarios dominate and the APDP is similar to the IPDP. Hence, presented gains for MLSE-C1 and MLSE-C2 based on instantaneous energy values, show a high potential of this approach for many UWB LDR applications.

c) Non-ideal Low Pass Filtering: By now the integration unit was idealized by a rectangular integration window. But to achieve an ultra low power consumption, the integration

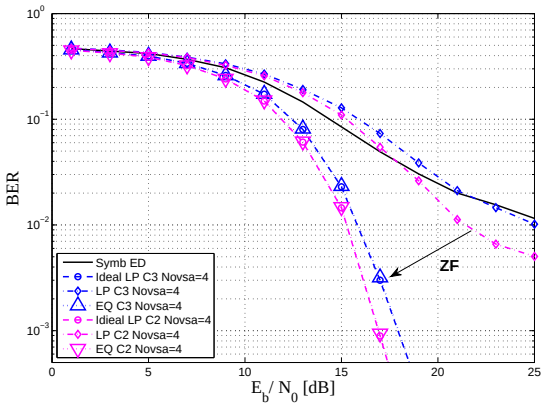

Fig. 4. BER performance with first order LP filter of 20 MHz bandwidth and ZF equalizer

window is preferably realized by a simple first order low pass filter [1]. In order to enable a reasonable integration duration and hence, to relax synchronization requirements, a small bandwidth is required. This introduces ISI. In Section IV, we showed that by a simple ZF equalizer of only a few samples the ISI can be canceled almost entirely. In Fig. 4, this is shown for moderate ISI with $\tau = 14$ ns, an over-sampling factor of $N_{\text{ovsa}} = 4$ and LP filter bandwidth $B = 20$ MHz. By application of the first order LP filter the performance degrades significantly up to 5 dB due to strong ISI. However, the ISI is entirely removed again by the simple ZF equalizer.

VII. Conclusions

A promising low complexity MLSE post-detection approach for ISI mitigation was investigated. Its potential was estimated by benchmarking it to optimal MLSE metrics derived for APDP and IPDP knowledge. It was shown that the presented MLSE approach again improves significantly, if marginal over-sampling is applied. Furthermore, the loss from Gaussian approximation and neglected cross-correlations was estimated below 3 dB. A simple ZF equalizer was presented which effectively cancels ISI introduced by a realistic LP filters and therefore, makes the proposed post-detection a valuable scheme for future ultra low power transceivers.

References

[1] F. Troesch, C. Steiner, T. Zasowski, T. Burger, and A. Wittneben, "Hardware aware optimization of an ultra low power UWB communication system," in *IEEE Int. Conf. Ultra-Wideband (ICUWB)*, Singapore City, Singapore, September 24 – 26, 2007.

[2] F. Troesch and A. Wittneben, "MLSE post-detection for ISI mitigation and synchronization in UWB low complexity receivers," in *IEEE Veh. Tech. Conf.*, Dublin, Ireland, 2006.

[3] T. Zasowski, F. Troesch, and A. Wittneben, "Partial channel state information and intersymbol interference in low complexity UWB PPM detection," in *IEEE Int. Conf. Ultra-Wideband (ICUWB)*, Waltham, MA, September 24 – 27, 2006.

[4] J. R. Barry, "Sequence detection and equalization for pulse-position modulation," in *Proc. ICC*, vol. 3, New Orleans, LA, May 1–5, 1994, pp. 1561 – 1565.

[5] M. Sahin and H. Arslan, "Inter-symbol interference in high data rate UWB communications using energy detector receivers," in *IEEE Int. Conf. Ultra-Wideband (ICU)*, Zurich, Switzerland, Sept. 5 – 8, 2005.